Inorg. Chem. **2006**, *45*, 7806–7814

Lanthanide Triple-Stranded Helicates: Controlling the Yield of the Heterobimetallic Species

Thomas B. Jensen, Rosario Scopelliti, and Jean-Claude G. BÜnzli*

Laboratory of Lanthanide Supramolecular Chemistry, École Polytechnique Fédérale de Lausanne, BCH 1402, CH-1015 Lausanne, Switzerland

Received May 17, 2006

Two unsymmetrical ditopic hexadentate ligands designed for the simultaneous recognition of two different trivalent lanthanide ions have been synthesized, L^{AB2} and L^{AB3}, where A represents a tridentate benzimidazole-pyridine-benzimidazole coordination unit, B2 a diethylamine-substituted benzimidazole-pyridine-carboxamide one, and B3 a chlorine-substituted benzimidazole-pyridine-carboxamide moiety. Under stoichiometric 2:3 (Ln/L) conditions, these ligands self-assemble with lanthanide ions to yield triple-stranded bimetallic helicates. The crystal structures of four helicates with L^{AB3} of composition $[LnLn'(L^{AB3})_3](ClO_4)_6 \cdot solv$ (CeCe, PrPr, PrLu, NdLu) show the metal ions embedded into a helical structure with a pitch of about 13.2–13.4 Å. The metal ions lie at a distance of 9.1–9.2 Å and are nine-coordinated by the three ligand strands, which are oriented in a HHH (head–head–head) fashion, where all ligand strands are oriented in the same direction. In the presence of a pair of different lanthanide ions in acetonitrile solution, the ligand L^{AB3} shows selectivity and gives high yields of heterobimetallic complexes. L^{AB2} displays less selectivity, and this is shown to be directly related to the tendency of this ligand to form high yields of HHT (head–head–tail) isomer. A fine-tuning of the HHH ⇆ HHT equilibrium and of the selectivity for heteropairs of Ln^{III} ions is therefore at hand.

Introduction

The programming of double- or triple-stranded helicates[1,2] containing two or three d transition metal ions is relatively easy in view of the substantial steric requirements of these ions. On the other hand, trivalent 4f ions have their valence orbitals shielded by the $5s^25p^6$ filled subshells and display, therefore, less specific steric requirements. Nevertheless, Piguet et al. demonstrated in 1992 that a carefully designed bis(tridentate) ligand based on bis(benzimidazole)pyridine and featuring two N_3 coordination units (L^A, Chart 1) yields, under stoichiometric conditions and by strict self-assembly, bimetallic triple-stranded lanthanide-containing helicates with a sizable stability in acetonitrile.[3] The corresponding heterobimetallic edifices display terbium-to-europium directional energy transfer.[4] The initial ligand design, tailored to induce a nine-coordinate, tricapped trigonal prismatic environment around the 4f ions, proved to be quite versatile and is amenable to easy modifications:[5,6] (i) the terminal benzimidazole moieties can be replaced by amide (L^B, Chart 1)[7] or carboxylic acid (L^C, Chart 1)[8] functions, the latter allowing the helicates to form in water; (ii) the 4-position of the pyridine rings can be substituted by Cl or Br,[9] opening the way to the grafting of groups able to couple with biological material;[10] (iii) expansion of the ligand frame to three and four tridentate coordination units leads to the isolation of homo-[11] and hetero-trimetallic,[12] as well as homo-tetrametallic,[13] triple-stranded helicates; (iv) reduction of the denticity of one coordinating group yields receptors able to

* To whom correspondence should be addressed. E-mail: jean-claude.bunzli@epfl.ch.

(1) Albrecht, M. *Chem. Rev.* **2001**, *101*, 3457−3497.
(2) Piguet, C.; Bernardinelli, G.; Hopfgartner, G. *Chem. Rev.* **1997**, *97*, 2005−2062.
(3) Bernardinelli, G.; Piguet, C.; Williams, A. F. *Angew. Chem., Int. Ed. Engl.* **1992**, *31*, 1622−1624.
(4) Piguet, C.; Bünzli, J.-C. G.; Bernardinelli, G.; Hopfgartner, G.; Williams, A. F. *J. Am. Chem. Soc.* **1993**, *115*, 8197−8206.
(5) Piguet, C.; Bünzli, J.-C. G. *Chem. Soc. Rev.* **1999**, *28*, 347−358.
(6) Bünzli, J.-C. G.; Piguet, C. *Chem. Rev.* **2002**, *102*, 1897−1928.
(7) Martin, N.; Bünzli, J.-C. G.; McKee, V.; Piguet, C.; Hopfgartner, G. *Inorg. Chem.* **1998**, *37*, 577−589.
(8) Elhabiri, M.; Scopelliti, R.; Bünzli, J.-C. G.; Piguet, C. *J. Am. Chem. Soc.* **1999**, *121*, 10747−10762.
(9) Platas, C.; Elhabiri, M.; Hollenstein, M.; Bünzli, J.-C. G.; Piguet, C. *J. Chem. Soc., Dalton Trans.* **2000**, 2031−2043.
(10) Tripier, R.; Hollenstein, M.; Elhabiri, M.; Chauvin, A.-S.; Zucchi, G.; Piguet, C.; Bünzli, J.-C. G. *Helv. Chim. Acta* **2002**, *85*, 1915−1929.
(11) Floquet, S.; Ouali, N.; Bocquet, B.; Bernardinelli, G.; Imbert, D.; Bünzli, J.-C. G.; Hopfgartner, G.; Piguet, C. *Chem. Eur. J.* **2003**, *9*, 1860−1875.
(12) Floquet, S.; Borkovec, M.; Bernardinelli, G.; Pinto, A.; Leuthold, L.-A.; Hopfgartner, G.; Imbert, D.; Bünzli, J.-C. G.; Piguet, C. *Chem. Eur. J.* **2004**, *10*, 1091−1105.

10.1021/ic0608501 CCC: $33.50 © 2006 American Chemical Society
Published on Web 08/22/2006

Chart 1

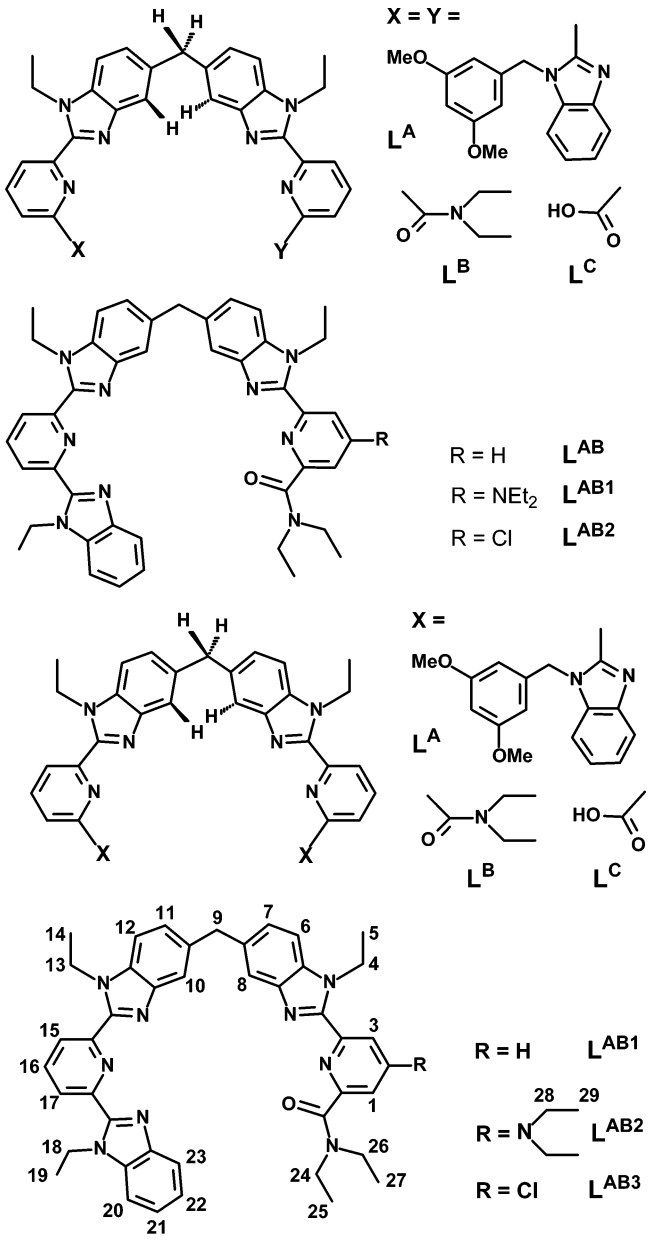

incorporate simultaneously a d and a 4f transition metal ion into the helical edifices,[14] e.g., in addition to Ln^{III}, Zn^{II},[15,16] Fe^{II},[17,18] Cr^{III},[19,20] and Ru^{II}.[19] In fact, only a few other lanthanide-containing helicates have been self-assembled with ligands based on different frameworks.[21−23]

There is presently an upsurge of interest in the development of luminescent lanthanide-containing probes for biomedical analysis and imaging in view of the specific spectroscopic properties of these ions.[24−26] In this context, increasing the number of detectable probes on a single sample, for instance, by designing stains with tunable emission wavelengths and simultaneously tunable excited-state lifetimes, is potentially interesting.[27] Bimetallic functional edifices may therefore combine two luminescent or one magnetic and one luminescent center in a single probe. The recognition of specific lanthanide ions in the presence of others is a difficult challenge in view of the limited differences in chemical properties and size of these ions (0.184 Å between La^{III} and Lu^{III} for coordination number 9, and 0.01−0.02 Å between two consecutive ions).[28] Several strategies can be adopted,[29] including "statistical crystallization", the design of guest molecules yielding sufficiently inert monometallic complexes to be reacted selectively with the second Ln^{III} ion, or self-assembly processes leading to the simultaneous recognition of a hetero pair of lanthanide ions. Using the latter approach, we have shown that the heteroditopic ligand L^{AB1} featuring N_3 and N_2O tridentate coordination sites (Chart 1) systematically leads to a sizable enhancement of the heterobimetallic species with respect to the statistical value, at least as soon as the ionic radius difference of the two Ln^{III} ions is larger than 0.1 Å. Another important result is that the selectivity is better when HHH (head−head−head; all three ligand strands oriented in the same direction) species form as compared to HHT (head−head−tail) helicates.[29]

To better understand the factors leading to selectivity for a hetero pair of Ln^{III} ions, we investigate here the effect of a modification of the N_2O tridentate binding unit (L^{AB2}, L^{AB3}, Chart 1) on the speciation in acetonitrile solution (hetero vs homo species, HHH vs HHT helicates). Structural data are also collected and discussed.

Experimental Section

Preparation of Ligands (Scheme 1, Scheme S1, Supporting Information). 4-Diethylamino-pyridine-2,6-dicarboxylic acid (**1**),[30] 4-chloro-6-(*N*,*N*-diethylcarbamoyl)pyridine-2-carboxylic acid (**5**),[9]

(13) Zeckert, K.; Hamacek, J.; Senegas, J.-M.; Dalla-Favera, N.; Floquet, S.; Bernardinelli, G.; Piguet, C. *Angew. Chem., Int. Ed.* **2005**, *44*, 7954−7958.
(14) Piguet, C.; Edder, C.; Rigault, S.; Bernardinelli, G.; Bünzli, J.-C. G.; Hopfgartner, G. *J. Chem. Soc., Dalton Trans.* **2000**, 3999−4006.
(15) Piguet, C.; Bünzli, J.-C. G.; Bernardinelli, G.; Hopfgartner, G.; Petoud, S.; Schaad, O. *J. Am. Chem. Soc.* **1996**, *118*, 6681−6697.
(16) Edder, C.; Piguet, C.; Bernardinelli, G.; Mareda, J.; Bochet, C. G.; Bünzli, J.-C. G.; Hopfgartner, G. *Inorg. Chem.* **2000**, *39*, 5059−5073.
(17) Edder, C.; Piguet, C.; Bünzli, J.-C. G.; Hopfgartner, G. *Chem. Eur. J.* **2001**, *7*, 3014−3024.
(18) Piguet, C.; Rivara-Minten, E.; Hopfgartner, G.; Bünzli, J.-C. G. *Helv. Chim. Acta* **1995**, *78*, 1651−1672.
(19) Torelli, S.; Imbert, D.; Cantuel, M.; Bernardinelli, G.; Delahaye, S.; Hauser, A.; Bünzli, J.-C. G.; Piguet, C. *Chem. Eur. J.* **2005**, *11*, 3228−3242.
(20) Cantuel, M.; Bernardinelli, G.; Imbert, D.; Bünzli, J.-C. G.; Hopfgartner, G.; Piguet, C. *J. Chem. Soc., Dalton Trans.* **2002**, 1929−1940.
(21) Bassett, A. P.; Magennis, S. W.; Glover, P. B.; Lewis, D. J.; Spencer, N.; Parsons, S.; Williams, R. M.; De Cola, L.; Pikramenou, Z. *J. Am. Chem. Soc.* **2004**, *126*, 9413−9424.
(22) Lessmann, J. J.; Horrocks, W. d., Jr. *Inorg. Chem.* **2000**, *39*, 3114−3124.
(23) Goodgame, D. M. L.; Hill, S. P. W.; Williams, D. J. *J. Chem. Soc., Chem. Commun.* **1993**, 1019−1021.
(24) Bünzli, J.-C. G.; Piguet, C. *Chem. Soc. Rev.* **2005**, *34*, 1048−1077.
(25) Faulkner, S.; Pope, S. J. A.; Burton-Pye, B. P. *Appl. Spectrosc. Rev.* **2005**, *40*, 1−31.
(26) Faulkner, S.; Matthews, J. L. In *Comprehensive Coordination Chemistry II*; Ward, M. D., Ed.; Elsevier Pergamon: Amsterdam, 2004; Vol. 9.21, pp 913−944.
(27) Chen, J. Y.; Selvin, P. R. *J. Am. Chem. Soc.* **2000**, *122*, 657−660.
(28) Bünzli, J.-C. G. *Acc. Chem. Res.* **2006**, *39*, 53−61.
(29) André, N.; Jensen, T. B.; Scopelliti, R.; Imbert, D.; Elhabiri, M.; Hopfgartner, G.; Piguet, C.; Bünzli, J.-C. G. *Inorg. Chem.* **2004**, *43*, 515−529.
(30) Achremowicz, L.; Mlochowski, J.; Mora, C.; Skarzewski, J. *Z. Prakt. Chem.* **1982**, *324*, 735−742.

Scheme 1

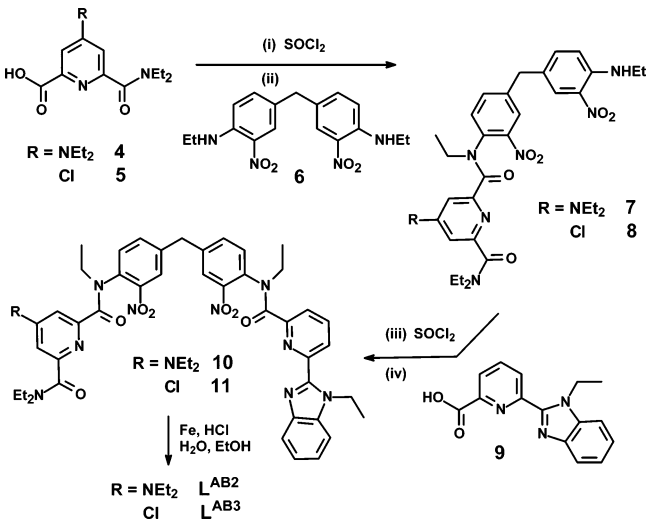

3,3′-dinitro-4,4′-bis(*N*-ethylamino)diphenylmethane (**6**),[31] and 6-(1-ethylbenzimidazol-2-yl)pyridine-2-carboxylic acid (**9**)[8] were prepared according to literature procedures.

Solvents and starting materials were purchased from Fluka A. G. (Buchs, Switzerland) and used without further purification, unless otherwise stated. Acetonitrile, dichloromethane, *N*,*N*-dimethylformamide (dmf), and triethylamine were distilled from CaH_2; thionyl chloride was distilled from elemental sulfur. Silica gel (Merck 60, 0.04−0.06 mm) was used for preparative column chromatography. Duplicate elemental analyses were performed by Dr. H. Eder from the Microchemical Laboratory of the University of Geneva.

Synthesis of 4-Diethylamino-6-methoxycarbonylpyridine-2-carboxylic Acid (2). A mixture of **1** (4.76 g; 20.0 mmol), 10 mL of H_2O, 50 mL of CH_3OH, and 2 mL of 97% H_2SO_4 was refluxed for 4 h, cooled to room temperature, and poured slowly into 160 mL of saturated $NaHCO_3$ solution. The solution was extracted with CH_2Cl_2 (3 × 50 mL). The aqueous phase was then acidified to pH 3 with 25% HCl and extracted with CH_2Cl_2 (12 × 50 mL) over the next 24 h. The extracts were dried over Na_2SO_4, filtered, and evaporated. Yield: 2.100 g (39%). TLC (CH_2Cl_2/CH_3OH = 95:5): R_f = 0.05. ^{1}H NMR (CD_3OD): δ 7.55 (d, 1H, ^4J = 2.9 Hz), 7.50 (d, 1H, ^4J = 2.9 Hz), 4.07 (s, 3H), 3.72 (q, 4H, ^3J = 7.2 Hz), 1.31 (t, 6H, ^3J = 7.2 Hz). MS (CH_3CN) *m*/*z*: 253.4 ([M + H]$^+$, calcd 253.3).

Synthesis of 4-Diethylamino-6-methoxycarbonylpyridine-2-(*N*,*N*-diethylcarbamoyl)pyridine (3) and 4-Diethylamino-2-(*N*,*N*-diethylcarbamoyl)pyridine-6-carboxylic Acid (4). After refluxing a solution of **2** (4.203 g; 16.66 mmol), $SOCl_2$ (30 mL; 412 mmol), and 0.1 mL of dmf in 100 mL of dry CH_2Cl_2 under an atmosphere of N_2 for 2 h, the solvent was evaporated, excess $SOCl_2$ was removed in a vacuum, and the residue was dried in a vacuum for 60 min. The pale yellow solid was redissolved in 100 mL of dry CH_2Cl_2; $HNEt_2$ (16 mL; 153 mmol) was added dropwise and the reaction mixture was refluxed under N_2 for 2 h. Following removal of solvent, the residue was partitioned between 150 mL of CH_2Cl_2 and 150 mL of NH_4Cl 3 M. The aqueous phase was extracted with CH_2Cl_2 (2 × 150 mL) and the combined organic phases were then washed with saturated $NaHCO_3$ (2 × 100 mL) and evaporated to yield crude **3**. This was dissolved in a mixture of 50 mL of CH_3OH and 50 mL of 1 M KOH and stirred overnight. Following removal of CH_3OH, the solution was extracted with CH_2Cl_2 (3 × 50 mL) and acidified to pH 1.6 with 25% HCl. The solution was then extracted with CH_2Cl_2 (13 × 50 mL) over the next 3 days. The combined extracts were dried over Na_2SO_4, filtered, and evaporated to yield 2.834 g (58%) of **4**. ^{1}H NMR (CD_3OD): δ 7.48 (d, 1H, ^4J = 2.8 Hz), 7.00 (d, 1H, ^4J = 2.8 Hz), 3.67 (q, 4H, ^3J = 7.2 Hz), 3.58 (q, 2H, ^3J = 7.2 Hz), 1.29 (t, 9H, ^3J = 7.2 Hz), 1.20 (t, 3H, ^3J = 7.2 Hz). ^{1}H NMR ($CDCl_3$): δ 7.44 (d, 1H, ^4J = 2.6 Hz), 6.82 (d, 1H, ^4J = 2.6 Hz), 3.57 (q, 2H, ^3J = 7.3 Hz), 3.49 (q, 4H, ^3J = 7.3 Hz), 3.33 (q, 2H, ^3J = 7.3 Hz), 1.29 (t, 3H, ^3J = 6.9 Hz), 1.24 (t, 6H, ^3J = 7.1 Hz), 1.20 (t, 3H, ^3J = 6.8 Hz). MS (CH_3CN): *m*/*z* 293.8 ([M + H]$^+$, calcd 294.2). Anal. Calcd for **4**, $C_{15}H_{23}N_3O_3$·0.5H_2O: C, 59.58; H, 8.00; N 13.90. Found C, 59.83; H, 7.80; N, 13.91.

Synthesis of Compound 7. A solution of **4** (549 mg; 1.87 mmol), $SOCl_2$ (5 mL; 69 mmol), and dmf (0.1 mL) in 50 mL of dry CH_2Cl_2 was refluxed under N_2 for 60 min. After removal of solvent and excess $SOCl_2$ in a vacuum, the residue was dried in a vacuum for 90 min and suspended in 30 mL of dry CH_2Cl_2. A solution of **6** (645 mg; 1.87 mmol) and NEt_3 (3 mL; 22 mmol) in 30 mL of dry CH_2Cl_2 was added slowly, and the reaction mixture was refluxed for 90 min. After evaporation to dryness, the residue was partitioned between 30 mL of CH_2Cl_2 and 30 mL of NH_4Cl 3 M solution. The aqueous phase was then extracted with CH_2Cl_2 (2 × 30 mL), and the combined organic phases were dried over Na_2SO_4, filtered, and evaporated to dryness. The crude product was purified on column (silica gel, CH_2Cl_2/CH_3OH = 100:0 → 97:3). Yield: 465 mg (40%). MS (CH_3OH) *m*/*z*: 620.4 ([M + H]$^+$, calc. 620.4). ^{1}H NMR ($CDCl_3$): δ 8.00 (d, 1H, ^4J = 1.9 Hz), 7.95 (s, 1H), 7.71 (d, 1H, ^4J = 1.7 Hz), 7.23 (m, 2H), 7.07 (d, 1H, ^3J = 8.0 Hz), 6.97 (d, 1H, ^4J = 2.4 Hz), 6.87 (d, 1H, ^3J = 8.9 Hz), 6.44 (d, 1H, ^4J = 2.5 Hz), 4.33 (sextet, 1H, ^3J = 7.1 Hz), 3.90 (s, 2H), 3.35−3.60 (m, 4H), 3.31 (q, 4H, ^3J = 7.3 Hz), 3.24 (sextet, 1H, ^3J = 6.9 Hz), 3.16 (sextet, 1H, ^3J = 7.2 Hz), 2.99 (sextet, 1H, ^3J = 7.2 Hz), 1.35 (t, 3H, ^3J = 7.2 Hz), 1.23 (t, 3H, ^3J = 7.2 Hz), 1.15 (t, 3H, ^3J = 7.2 Hz), 1.10 (t, 6H, ^3J = 7.1 Hz), 0.90 (t, 3H, ^3J = 7.1 Hz).

Synthesis of Compound 8. A solution of **5** (1.40 g; 5.45 mmol), 10 mL of $SOCl_2$, and 0.1 mL of dmf in 40 mL of dry CH_2Cl_2 was refluxed under N_2 for 60 min. After evaporation, the residue was dried in a vacuum at 40 ° C for 75 min and then redissolved in 30 mL of dry CH_2Cl_2. A solution of **3** (1.87 g; 5.43 mmol) and 5 mL of NEt_3 in 30 mL of dry CH_2Cl_2 was added. The solution was then stirred at room temperature for 40 min and refluxed for 70 min under nitrogen. After evaporation of the solvent, the residue was partitioned between 50 mL of NH_4Cl 3 M and 50 mL of CH_2Cl_2. The aqueous phase was extracted twice with 50 mL of CH_2Cl_2, and the combined organic phases were dried over Na_2SO_4, filtered, and evaporated to dryness. The resulting residue was purified on column (silica; CH_2Cl_2/CH_3OH= 100:0 → 98:2) to yield 2.089 g of **8** (66%). MS: *m*/*z* = 583.3 [M + H]$^+$ (calc. 583.2). 1H NMR ($CDCl_3$): δ 8.02 (d, 1H, ^4J = 2.1 Hz), 7.97 (s br, 1H), 7.83 (d, 1H, ^4J = 1.8 Hz), 7.76 (d, 1H, ^4J = 2.0 Hz), 7.35 (d, 1H, ^4J = 2.0 Hz), 7.25 (dd, 1H, ^3J = 8.4 Hz, ^4J = 2.0 Hz), 7.22 (dd, 1H, ^3J = 9.2 Hz, ^4J = 2.1 Hz), 7.03 (d, 1H, ^3J = 8.1 Hz), 6.89 (d, 1H, ^3J = 8.8 Hz), 4.34 (sextet, 1H, ^3J = 7.1 Hz), 3.92 (s, 2H), 3.56 (sextet, 1H, ^3J = 7.1 Hz), 3.55 (sextet, 1H, ^3J = 7.1 Hz), 3.37 (sextet, 1H, ^3J = 7.1 Hz), 3.35 (sextet, 1H, ^3J = 7.1 Hz), 3.29 (sextet, 1H, ^3J = 6.9 Hz), 3.14 (sextet, 1H, ^3J = 7.3 Hz), 2.98 (sextet, 1H, ^3J = 7.3 Hz), 1.38 (t, 3H, ^3J = 7.2 Hz), 1.25 (t, 3H, ^3J = 7.3 Hz), 1.17 (t, 3H, ^3J = 7.2 Hz), 0.93 (t, 3H, ^3J = 7.1 Hz).

Synthesis of Compound 10. A solution of **9** (267 mg; 1 mmol), $SOCl_2$ (3 mL; 41 mmol), and dmf (0.1 mL) in 50 mL of dry CH_2Cl_2 was refluxed under N_2 for 60 min. After removal of solvent

(31) Piguet, C.; Bernardinelli, G.; Bocquet, B.; Quattropani, A.; Williams, A. F. *J. Am. Chem. Soc.* **1992**, *114*, 7440−7451.

and excess $SOCl_2$ in a vacuum, the residue was dried in a vacuum for 40 min and suspended in 30 mL of dry CH_2Cl_2. A solution of **7** (553 mg; 0.89 mmol) and NEt_3 (2 mL, 14 mmol) in 30 mL of dry CH_2Cl_2 was added slowly, and the reaction mixture was refluxed for 90 min. After evaporation to dryness, the residue was partitioned between 25 mL of CH_2Cl_2 and 25 mL of NH_4Cl 3 M. The aqueous phase was then extracted with CH_2Cl_2 (2 × 25 mL), and the combined organic phases were dried over Na_2SO_4, filtered, and evaporated to dryness. The crude product was purified on column (silica gel, CH_2Cl_2/CH_3OH = 100:0 → 97:3). Yield: 424 mg (49%). MS (CH_3OH) *m*/*z*: 868.8 ($[M + H]^+$, calcd 869.4), 891.4 ($[M + Na]^+$, calcd 891.4), 435.3 ($[M + 2H]^{2+}$, calcd 435.2).

Synthesis of Compound 11. A solution of **9** (1.036 g; 3.87 mmol), 10 mL of $SOCl_2$, and 0.1 mL of dmf in 40 mL of dry CH_2Cl_2 was refluxed under nitrogen for 55 min. After evaporation, the residue was dried in a vacuum at 40 °C for 80 min and then suspended in 25 mL dry CH_2Cl_2. A solution of **8** (2.26 g; 3.87 mmol) and 5 mL of NEt_3 in 30 mL of dry CH_2Cl_2 was added dropwise. The solution was then refluxed for 2 h under nitrogen. After evaporation, the residue was partitioned between 50 mL of NH_4Cl 3 M and 50 mL of CH_2Cl_2. The aqueous phase was extracted twice with 35 mL of CH_2Cl_2, and the combined organic phases were dried over Na_2SO_4, filtered, and evaporated to dryness. The resulting residue was purified on column (silica; CH_2Cl_2/CH_3OH = 100:0 → 98:2) to yield 1.508 g of **11** (47%). MS: *m*/*z* = 832.3 $[M + H]^+$ (calcd 832.3).

Synthesis of Ligand L^{AB2}. A mixture of **10** (403 mg; 0.46 mmol), Fe powder (0.80 g; 14 mmol), EtOH (30 mL), H_2O (10 mL), and 25% HCl (5 mL) was refluxed under N_2 for 18 h. After removal of EtOH, the solution was mixed with 60 mL of CH_2Cl_2 and a solution of H_4-edta (35 g; 120 mmol) and NaOH (16 g; 0.4 mol) in 150 mL of H_2O was added. The solution was neutralized with 5 M KOH and 4 mL 30% H_2O_2 was added after which the pH was adjusted to 8.5 with 5 M KOH. After stirring for 30 min, the organic phase was separated and the aqueous phase was extracted with CH_2Cl_2 (3 × 50 mL). The combined organic phases were dried over Na_2SO_4, filtered, and evaporated to dryness. The crude product was purified on column (silica gel, CH_2Cl_2/CH_3OH = 100:0 → 95:5). The product was washed with pentane and dried in a vacuum. Yield: 240 mg (67%). MS (CH_3OH) *m*/*z*: 773.3 ($[M + H]^+$, calcd 773.4), 794.9 ($[M + Na]^+$, calcd 795.4). Anal. Calcd for $C_{47}H_{52}N_{10}O{\cdot}0.5H_2O$: C, 72.19; H, 6.83; N 17.91. Found C, 72.02; H, 6.72; N, 17.90. See Table S1 (Supporting Information) for assignment of ^1H NMR spectrum in $CDCl_3$.

Synthesis of Ligand L^{AB3}. A mixture of **11** (1.453 g; 1.75 mmol), Fe powder (3.00 g; 53.7 mmol), 20 mL of 25% HCl, 20 mL of water, and 90 mL of ethanol was refluxed under nitrogen overnight. After removal of ethanol, the reaction mixture was poured into a solution of 70 g of H_4-edta and 30 g of NaOH in 200 mL of water. To this was added 20 mL of 30% H_2O_2, the pH was adjusted to 8.5 with 5 M KOH, 75 mL of CH_2Cl_2 was added, and the mixture was stirred for 30 min. The two phases were separated, and the red aqueous phase was extracted three times with 75 mL of CH_2Cl_2. The combined organic phases were dried over Na_2SO_4, filtered, and evaporated to dryness. The crude product was purified on column (silica; CH_2Cl_2/CH_3OH = 100:0 → 96:4) to yield 945 mg of L^{AB3} (73%). MS: *m*/*z* = 736.4 $[M + H]^+$ (calcd 736.3). Anal. Calcd for $C_{43}H_{42}N_9OCl{\cdot}0.5H_2O$: C, 69.29; H, 5.82; N 16.91. Found C, 69.17; H, 5.80; N, 16.84. See Table S2 (Supporting Information) for assignment of ^1H NMR spectrum in $CDCl_3$.

Preparation of the Complexes $[Ln_2(L)_3](ClO_4)_6$ and $[LnLn'(L)_3](ClO_4)_6$. Partially dehydrated perchlorate salts $Ln(ClO_4)_3{\cdot}xH_2O$ (Ln = La−Lu, *x* = 2−4) were prepared from the corresponding oxides (Rhône-Poulenc, 99.99%) in the usual way.[32] ***Caution:*** *Perchlorate salts combined with organic ligands are potentially explosive and should be handled in small quantities and with adequate precautions!*[33] Stock solutions of $Ln(ClO_4)_3{\cdot}xH_2O$ in CH_3CN were prepared by weighting. The concentrations of the solutions were determined by complexometric titrations with $Na_2(H_2edta)$ in the presence of urotropine using xylene orange as indicator.

NMR samples of homobimetallic $[Ln_2(L)_3](ClO_4)_6$ complexes were prepared by reacting a weighed amount of L (3−15 mg) dissolved in CH_2Cl_2 with 2/3 equiv of $Ln(ClO_4)_3{\cdot}xH_2O$ in the form of a CH_3CN solution. After stirring for 1−3 h, the solution was evaporated to dryness, the residue was dried in a vacuum at 50 °C, and redissolved in 0.6 mL CD_3CN. Samples of heterobimetallic $[LnLn'(L)_3](ClO_4)_6$ complexes were prepared in an analogous way using 1/3 equiv of $Ln(ClO_4)_3$ and 1/3 equiv of $Ln'(ClO_4)_3$ and stirring the sample overnight before evaporation.

Solid samples of homobimetallic triple helicate complexes of L^{AB3} were obtained by reacting 2/3 equiv of $Ln(ClO_4)_3$ with L^{AB3} (5−15 mg) in CH_3CN solution. In a similar way, heterobimetallic complexes were obtained by reacting 1/3 equiv of $Ln(ClO_4)_3$ and 1/3 equiv of $Ln'(ClO_4)_3$ with the ligand. After evaporation to dryness and drying in a vacuum, the solid residues were redissolved in a 1:1 CH_3CN/CH_3CH_2CN mixture (≈0.5 mL) and precipitated by slow diffusion of ^{t}BuOMe at $T = -18$ °C.

Spectroscopic Measurements. MS spectra used for the characterization of organic compounds were recorded in CH_3OH or CH_3CN with a Finnigan SSQ-710C spectrometer. 1D ^1H NMR spectra, as well as 2D COSY and ROESY experiments, were performed on Bruker Avance 400 (400 MHz) and 600 (600 MHz) spectrometers.

X-ray Crystallographic Data. Data collection was carried out at 140(2) K on a four-circle goniometer having κ geometry and equipped with an Oxford Diffraction KM4 Sapphire CCD (all helicates but $[Ce_2(L^{AB3})_3](ClO_4)_6$) or a mar345 IPDS. Data reduction was performed with CrysAlis RED, release 1.7.0.[34] In two cases, data have been corrected for absorption. Structure solution and refinement were performed with the SHELXTL software, release 5.1.[35] The structures were refined using the full-matrix-block least-squares on F^2 with all non-H atoms refined anisotropically. H atoms were placed in calculated positions with the "riding" model. The solvent molecules have been retained as isotropic.

All the crystals were weakly diffracting samples (see the number of observed reflections compared to the number of unique reflections), the number of refined parameters is very high (about 1900), and the anions and solvent molecules show extensive disorder. This explains the relatively high values of R1, particularly for the Ce_2 compound.

Results

Ligand Design, Synthesis, and Properties. In previous work, we have shown that the unsymmetrical ditopic ligand L^{AB1} allows the simultaneous recognition of two Ln^{III} ions differing in ionic radius by more than 0.1 Å, the percentage of heterobimetallic species reaching 90% for the $La^{III}-Lu^{III}$ pair ($[LaLu(L^{AB1})_3]^{6+}$ or $LaLu(L^{AB1})_3$, as here and in the

(32) Desreux, J. F. In *Lanthanide Probes in Life, Chemical and Earth Sciences. Theory and Practice*; Bünzli, J.-C. G., Choppin, G. R., Eds.; Elsevier Science Publishers B. V.: Amsterdam, 1989; Vol. 2, pp 43−64.
(33) Raymond, K. N. *Chem. Eng. News* **1983**, *61*, 4.
(34) *CrysAlis RED*, version 1.7.0; Oxford Diffraction Ltd.: Abingdon, UK, 2003.
(35) *SHELXTL*, release 5.1; Bruker AXS, Inc.: Madison, WI, 1997.

Table 1. Crystallographic Data for $[LnLn'(L^{AB3})_3](ClO_4)_6 \cdot x CH_3CN \cdot y CH_3CH_2CN$

	Ce_2	Pr_2	PrLu	NdLu
x; *y*	5; 2	6; 4	7; 3	5; 2
formula	$C_{145}H_{151}Ce_2Cl_9N_{34}O_{27}$	$C_{153}H_{164}Cl_9N_{37}O_{27}Pr_2$	$C_{152}H_{162}Cl_9LuN_{37}O_{27}Pr$	$C_{145}H_{151}Cl_9LuN_{34}NdO_{27}$
mol weight	3401.29	3554.08	3574.12	3440.26
temp (K)	140(2)	140(2)	140(2)	140(2)
cryst syst	monoclinic	triclinic	triclinic	monoclinic
space group	$P2_1/n$	$P\bar{1}$	$P\bar{1}$	$P2_1/n$
a (Å)	30.819(10)	15.0272(13)	15.0634(11)	30.992(3)
b (Å)	15.113(2)	19.214(2)	19.3270(18)	15.0821(9)
c (Å)	34.771(11)	30.105(2)	30.237(2)	34.666(3)
α (deg)	90	103.87(1)	104.10(1)	90
β (deg)	109.79(3)	101.42(1)	100.84(1)	109.251(7)
γ (deg)	90	95.75(1)	96.22(1)	90
V (Å^3)	15238.71(700)	8171.42(130)	8274.88(110)	15297(2)
F(000)	6976	3656	3664	7036
Z	4	2	2	4
D_c (Mg·m^{-3})	1.482	1.444	1.434	1.494
μ(Mo Kα) (mm^{-1})	0.830	0.817	1.108	1.216
cryst size (mm^3)	0.35 × 0.31 × 0.15	0.30 × 0.19 × 0.15	0.30 × 0.19 × 0.15	0.35 × 0.31 × 0.15
reflns measured	81 966	48 975	49 646	87 058
unique reflns	25 902	25 306	25 563	25 615
no. of params	1901	1839	1880	1883
constraints	679	687	680	679
GOF on F^2 [b]	0.927	0.796	0.854	0.878
R1 [$I > 2\sigma(I)$][a]	0.1175	0.0816	0.0787	0.0933
wR2[a]	0.3923	0.2346	0.2317	0.3022

[a] $R1 = \sum||F_o| - |F_c||/\sum|F_o|$, $wR2 = \{\sum[w(F_o^2 - F_c^2)^2]/\sum[w(F_o^2)^2]\}^{1/2}$. [b] $GOF = \{\sum[w(F_o^2 - F_c^2)^2]/(n-p)\}^{1/2}$.

following charges of complexes will be omitted for clarity).[29] The ligand design called for combining one tridentate unit, benzimidazole-pyridine-benzimidazole (bpb) constructed from L^1 (Chart 1) which features a peculiar behavior toward lanthanide ions with a stability maximum for the lighter Ln^{III} ions,[36] and another tridentate unit including a diethylamide group (L^{2b}, Chart 1) which produces a commonly observed increase in stability along the lanthanide series.[37,38]

The addition of substituents on the 4-position of one of the pyridyl groups in the present work was done to slightly modify the electron density on the ligating nitrogen atom and to test its effect on the selectivity for heteropairs of Ln^{III} ions. The electron-donating NEt_2 group in L^{AB2} was expected to increase the electron density and thus increase the affinity of the benzimidazole-pyridine-amide coordinating unit (bpa) toward the heavier Ln^{III} ions, leading to better selectivity toward a pair of different Ln^{III} ions. The weakly electron withdrawing Cl substituent in L^{AB3}, on the other hand, is expected to give a slight opposite effect.

The ligands L^{AB2} and L^{AB3} were obtained in reasonably good yields using strategies developed for ligands L^{AB1} [29] and L^B. [7] The final step of the synthesis is a modified Phillips[39] reaction of the intermediates **10** and **11**, obtained by consecutive reaction of **6** with **4** (L^{AB2}) or **5** (L^{AB3}) followed by **9** (Scheme 1).

^{1}H NMR spectroscopy (1D, COSY, and ROESY) in $CDCl_3$ showed that the ligands adopt the usual trans conformation.[8] This is concluded on the basis of the absence of NOE signals between pyridyl protons (H1, H3, H15, H17, Chart 1) and methylene groups (H24/H26, H4, H13, and H18, respectively), indicating that the pyridyl groups are rotated in a fashion that places their N-donor atoms in a trans configuration with respect to the other ligating atoms (N and O) of the benzimidazole and carboxamide groups. This implies that complexation with a pair of Ln^{III} ions requires some conformational work to rotate the ligating atoms of each coordination unit to point in the same direction.

Isolation, Characterization, and Structure of the Helicates. Solid samples of the helicates could be made by slow diffusion of ^{t}BuOMe into a concentrated CH_3CN/CH_3CH_2CN (1:1) solution and gave satisfactory elemental analyses (Table S3, Supporting Information). Four samples yielded crystals of sufficient quality for X-ray diffraction studies (Table 1). In the monoclinic $Ce_2(L^{AB3})_3$ and $NdLu(L^{AB3})_3$, as well as in the triclinic $Pr_2(L^{AB3})_3$ and $PrLu(L^{AB3})_3$, structures, the unit cell contains isolated helical HHH-$[LnLn'(L^{AB3})_3]^{6+}$ molecular ions formed by two lanthanide ions and three ligand strands, perchlorate counterions, and solvent molecules (Figure 1). The molecular ions are present in the unit cell as a racemic mixture of the two P and M isomers.

In the two heterobimetallic structures, the smaller Lu^{III} ion is assigned to be in the bpa coordination cavity formed by the three ligand strands (Figure 2). For the PrLu compound, different models have been tried in order to check if this assumption is valid. The models Pr(bpb)Pr(bpa), Lu(bpb)Lu(bpa), Lu(bpb)Pr(bpa), and Pr(bpb)Lu(bpa) gave R1 values equal to 0.0816, 0.0853, 0.0943, and 0.0787, respectively, probably pointing to a correct assignment of the two lanthanide ions. This approach does, however, not take into account partial occupancy of the two sites. Attempts to refine the crystal structures with the occupancies treated as variables was unfortunately not possible due to the relatively low

(36) Petoud, S.; Bünzli, J.-C. G.; Renaud, F.; Piguet, C.; Schenk, K. J.; Hopfgartner, G. *Inorg. Chem.* **1997**, *36*, 5750−5760.
(37) Le Borgne, T.; Altmann, P.; André, N.; Bünzli, J.-C. G.; Bernardinelli, G.; Morgantini, P.-Y.; Weber, J.; Piguet, C. *J. Chem. Soc., Dalton Trans.* **2004**, 723−733.
(38) The stability constants given in ref 34 for complexes with L^{2b} are misquoted, and the correct data only include Eu^{III} and Lu^{III}. We refer instead to the stability constants of the closely related ligand L^{2a} given in the same reference.
(39) Phillips, M. A. *J. Chem. Soc.* **1928**, 172−177.

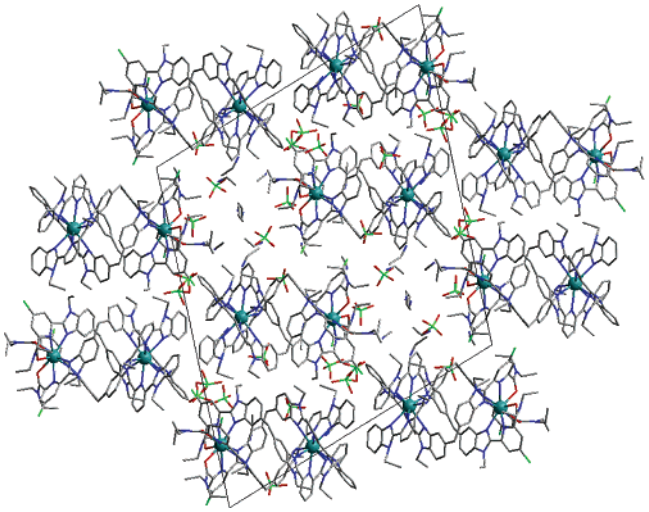

Figure 1. Structure of $[Ce_2(L^{AB3})_3](ClO_4)_6 \cdot 5CH_3CN \cdot 2CH_3CH_2CN$ viewed along the *b* axis.

Chart 2. Numbering of Ligating Atoms in Ligand Strands 1 (top), 2 (middle), and 3 (bottom)

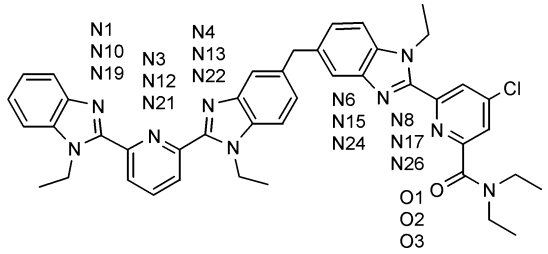

quality of the crystals. To better ascertain the heterometallic model, we have turned to a thorough analysis of the $Ln^{III}-X$ bond lengths.

In the benzimidazole-pyridine-benzimidazole coordination site, the $Pr^{III}-X$ bond lengths (Chart 2, Table 2) are similar to what was found for the closely related complexes with L^{AB1}. This is as expected since the bpb units are the same in the two ligands. The $Ce^{III}-X$ and $Nd^{III}-X$ distances are longer and shorter, respectively, a result of the lanthanide contraction. The bonds in the benzimidazole-pyridine-amide coordination site in the two homobimetallic complexes are all longer than the corresponding bonds in the Lu-containing helicates, also in line with the relative sizes of the ions. On the other hand, the bpa bond lengths are slightly longer than the corresponding bonds in the HHH-$[PrLu(L^{AB1})_3](ClO_4)_6$ compound. This could indicate that the site is partially occupied by the larger lanthanide ions in the complexes with Pr and Nd.

The coordination polyhedra around the two lanthanide ions (Figure 3) are slightly distorted tricapped trigonal prisms. The upper and lower faces of the prism are defined by the benzimidazole nitrogen atoms and (in the bpa unit) the amide oxygen atoms. The prisms are capped by the pyridine nitrogen atoms. The principal deviation from regular tricapped trigonal prisms is the angle ω, which describes the twist between the upper and lower faces of the prism. In the pba unit, this angle is 15(1)°, 14(2)°, 10.1(7)°, and 11.0(6)°, respectively, in the Ce_2, Pr_2, PrLu, and NdLu complexes. In the bpb unit, the values are 15(1)°, 15(3)°, 14(3)°, and 14(1)°. As can be seen, the value of ω decreases with decreasing ionic radius of the Ln^{III} ion, a behavior also observed for the complexes with L^{AB1}. A detailed analysis of the coordination polyhedra is given in Figure S1 and Tables S4, S5 (Supporting Information).

To further characterize the structure of the helicates, we have calculated the Ln−Ln′ distance as well as the pitch, *P*, the distance needed for the helix to make one complete turn (Table S6, Supporting Information). For all the complexes under investigation here, as well as for the related L^{AB1} complexes, the values found are remarkably similar, with *P* being 13.2−13.5 Å and *d*(Ln−Ln′) being in the range of 9.10−9.35 Å.

Least squares planes have been defined for the aromatic ring systems of the ligands, and the angles and distances between them have been calculated (Tables S7, S8, Supporting Information). Most of these planes are not parallel or close enough to conclude that there are $\pi-\pi$ interstrand interactions present, the only exception being imidazole groups in the bpb moiety of the ligand. Here, the shortest distance is 3.496(2) Å for two almost parallel planes (the angle is 9.1°). The presence of weak interstrand interactions was previously reported for bimetallic complexes of L^A (angles 14.8−21°; distances 3.7−4.6 Å)[4] and L^{AB1} (angles 11.5−33.9°; distances 3.7−4.0 Å).[29] This is in contrast to what was found for monometallic complexes of the related ligand L^1 (Chart 1), where the distances between almost parallel (9.1°) planes are 3.1−3.3 Å.[40]

Speciation in Acetonitrile. Acetonitrile solutions of complexes with L^{AB2} and L^{AB3} have been studied by means of ^1H NMR spectroscopy with a total ligand concentration of $10^{-3}-10^{-2}$ M. Under these experimental conditions, the only complexes present in solution are of general composition $[Ln_2(L)_3]^{6+}$ (2:3).

For homobimetallic complexes, two isomers are possible: HHH in which all three ligands are oriented in the same direction and the benzimidazole-pyridine-benzimidazole moieties are coordinated to the same lanthanide ion and HHT where one of the three ligand strands binds the benzimidazole-pyridine-benzimidazole moiety to the lanthanide ion which is coordinated by the benzimidazole-pyridine-amide moieties of the other two ligands. For the HHH isomer, the macroscopic formation constant, β_{LnLn}^{HHH}, is equal to $(k_{Ln}^{\alpha}) \times (k_{Ln}^{\beta}) \times (u^{HHH}) \times (u_{LnLn}^{HHH})$ where (k_{Ln}^{α}) and (k_{Ln}^{β}) are the absolute affinity constants of site α (the bpa-bpa-bpa site) and β (bpb-bpb-bpb), respectively, for Ln; u^{HHH} is the pre-organization energy (including attractive and repulsive interactions between ligand strands) for the formation of an "empty" triple helix from three ligands and u_{LnLn}^{HHH} describes the Ln−Ln (Coulomb) repulsion.[13,41−45] The similar constant for the HHT isomer, β_{LnLn}^{HHT}, can be written as $3 \times (k_{Ln}^{\gamma}) \times (k_{Ln}^{\delta}) \times (u^{HHT}) \times (u_{LnLn}^{HHT})$ where γ stands for the bpa-bpa-bpb site and δ is the bpa-bpb-bpb one; the factor 3 is the degeneracy. Thus, a total of eight parameters are necessary to describe the system if no simplifications are

(40) Piguet, C.; Williams, A. F.; Bernardinelli, G.; Bünzli, J.-C. G. *Inorg. Chem.* **1993**, *32*, 4139−4149.

Table 2. Ln^{III}−Donor Atom Distances in $[LnLn'(L^{AB3})_3](ClO_4)_6 \cdot x$MeCN$\cdot y$EtCN

	bpb unit							bpa unit					
	terminal benzimidazole		pyridine		bridging benzimidazole			bridging benzimidazole		pyridine		carboxamide	
Ce	N1	2.68(3)	N3	2.69(3)	N4	2.62(1)	Ce	N6	2.64(3)	N8	2.61(1)	O1	2.47(2)
$Ce_2(L^{AB3})_3$	N10	2.63(3)	N12	2.68(1)	N13	2.62(3)	$Ce_2(L^{AB3})_3$	N15	2.68(3)	N17	2.70(2)	O2	2.48(2)
	N19	2.68(2)	N21	2.67(1)	N22	2.64(2)		N24	2.65(3)	N26	2.66(1)	O3	2.44(4)
	mean	2.66(3)	mean	2.679(8)	mean	2.63(1)		Mean	2.66(2)	mean	2.66(4)	mean	2.46(2)
Pr	N1	2.65(1)	N3	2.66(2)	N4	2.64(2)	Pr	N6	2.70(2)	N8	2.69(2)	O1	2.48(1)
$Pr_2(L^{AB3})_3$	N10	2.62(2)	N12	2.61(2)	N13	2.68(2)	$Pr_2(L^{AB3})_3$	N15	2.60(1)	N17	2.68(2)	O2	2.47(1)
	N19	2.58(1)	N21	2.65(2)	N22	2.53(1)		N24	2.59(2)	N26	2.65(2)	O3	2.41(1)
	mean	2.62(4)	mean	2.64(3)	mean	2.62(8)		Mean	2.63(6)	mean	2.67(2)	mean	2.45(4)
Pr	N1	2.63(1)	N3	2.64(1)	N4	2.63(1)	Lu	N6	2.60(1)	N8	2.63(2)	O1	2.40(1)
$PrLu(L^{AB3})_3$	N10	2.63(1)	N12	2.63(1)	N13	2.66(1)	$PrLu(L^{AB3})_3$	N15	2.54(1)	N17	2.58(1)	O2	2.35(1)
	N19	2.62(1)	N21	2.64(2)	N22	2.55(1)		N24	2.55(1)	N26	2.55(1)	O3	2.31(1)
	mean	2.627(5)	mean	2.637(5)	mean	2.62(6)		Mean	2.56(3)	mean	2.59(4)	mean	2.35(5)
Nd	N1	2.63(1)	N3	2.67(1)	N4	2.60(1)	Lu	N6	2.59(1)	N8	2.58(1)	O1	2.40(1)
$NdLu(L^{AB3})_3$	N10	2.59(1)	N12	2.61(1)	N13	2.59(1)	$NdLu(L^{AB3})_3$	N15	2.62(1)	N17	2.61(1)	O2	2.37(1)
	N19	2.65(1)	N21	2.64(1)	N22	2.61(1)		N24	2.57(1)	N26	2.52(1)	O3	2.34(1)
	mean	2.63(3)	mean	2.64(3)	mean	2.60(1)		Mean	2.59(2)	mean	2.57(5)	mean	2.37(3)

made. If the four affinity constants were all the same, the pre-organization energies the same for the two isomers, and the two Ln−Ln repulsion parameters were equal, the equilibrium constant for the HHH ⇄ HHT isomerization would be 3, corresponding to a distribution of 25% HHH and 75% HHT. We will refer to this as the statistical distribution corresponding to the complexation of two identical lanthanide ions by a homobitopic ligand. Although this description is obviously oversimplified, it serves as a reference point in the later discussion.

In solution with overall heterobimetallic stoichiometry Ln/Ln′/L = 1:1:3, a total of eight different complexes can self-assemble. In addition to the four homobimetallic complexes, it is possible to form four different heterobimetallic complexes: HHH-LnLn′$(L)_3$, HHT-LnLn′$(L)_3$, HHH-Ln′Ln$(L)_3$, and HHT-Ln′Ln$(L)_3$, respectively. A more detailed description in terms of macroscopic formation constants as it was outlined for the homobimetallic complexes would require a total of 16 parameters: (k^{α}_{Ln}), (k^{β}_{Ln}), (k^{γ}_{Ln}), (k^{δ}_{Ln}), $(k^{\alpha}_{Ln'})$, $(k^{\beta}_{Ln'})$, $(k^{\gamma}_{Ln'})$, $(k^{\delta}_{Ln'})$, (u^{HHH}), (u^{HHT}), (u^{HHH}_{LnLn}), $(u^{HHH}_{LnLn'})$, $(u^{HHH}_{Ln'Ln'})$, (u^{HHT}_{LnLn}), $(u^{HHT}_{LnLn'})$, $(u^{HHT}_{Ln'Ln'})$.

The statistical distribution is 50% LnLn′, 25% Ln_2, and 25% Ln'_2. These percentages are, of course, not predictions, since they correspond to a situation where the ligand shows no selectivity toward a pair of lanthanide ions. The ligands under investigation here, on the other hand, are designed to display behavior deviating significantly from the statistical distribution.

Resonances in the homobimetallic (Ln/L = 2:3) NMR spectra have been attributed to the two possible isomers on the basis of the number of signals. In the HHH isomer, the three ligand strands are equivalent and give only one set of signals; for the HHT isomer, the three ligand strands each give one set of signals. This is illustrated in Figure 4, where partial spectra of the La_2 complexes of the two ligands are given. The spectrum of the L^{AB3} complex is particularly illustrative. In the spectral region included here, the HHH isomer only gives two signals (H8 and H10), both from aromatic protons that have been shifted out of the usual aromatic region of the spectrum because of the wrapping of

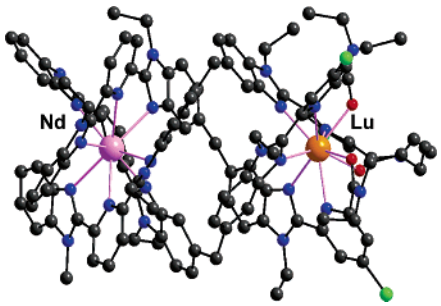

Figure 2. $[NdLu(L^{AB3})_3]^{6+}$ molecular ion (N atoms are in blue, O atoms in red, and Cl atoms in green).

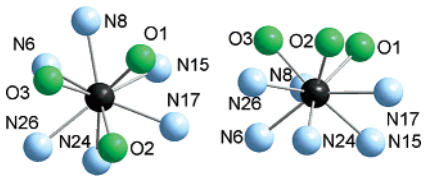

Figure 3. Two views of the bpa coordination polyhedron in the $Ce_2(L^{AB3})_3$ complex.

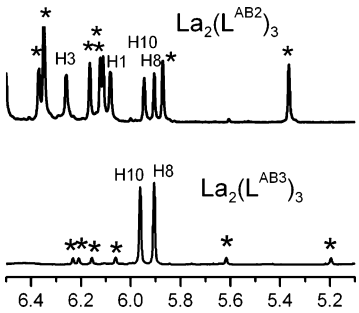

Figure 4. Partial NMR spectra. HHT signals are indicated with asterisks.

(41) Zeckert, K.; Hamacek, J.; Rivera, J. P.; Floquet, S.; Pinto, A.; Borkovec, M.; Piguet, C. *J. Am. Chem. Soc.* **2004**, *126*, 11589−11601.
(42) Borkovec, M.; Hamacek, J.; Piguet, C. *Dalton Trans.* **2004**, 4096−4105.
(43) Hamacek, J.; Borkovec, M.; Piguet, C. *Chem. Eur. J.* **2005**, *11*, 5217−5226.
(44) Piguet, C.; Borkovec, M.; Hamacek, J.; Zeckert, K. *Coord. Chem. Rev.* **2005**, *249*, 705−729.
(45) Hamacek, J.; Borkovec, M.; Piguet, C. *Dalton Trans.* **2006**, 1473−1490.

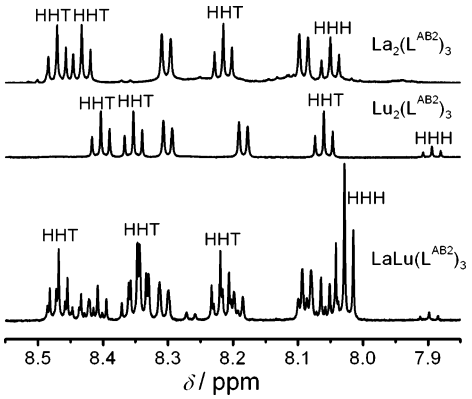

Figure 5. Partial 600 MHz ^{1}H NMR spectra of $La_2(L^{AB2})_3$ (top), $Lu_2(L^{AB2})_3$ (middle), and $LaLu(L^{AB2})_3$ (bottom) in CD_3CN solution. Signals assigned to H16 for the HHH and HHT isomers are indicated.

Table 3. Percentages of HHH Isomer

	L^{AB1}	L^{AB2}	L^{AB3}
$La_2(L)_3$	73	20	79
$Ce_2(L)_3$	69	13	79
$Pr_2(L)_3$	67	12	87
$Nd_2(L)_3$	69	15	87
$Sm_2(L)_3$	65	11	85
$Eu_2(L)_3$	69	8	85
$Y_2(L)_3$	63	8	82
$Lu_2(L)_3$	68	6	86

the ligand strands which places these protons close to a π-ring system. In the same spectral range, six signals are attributed to the HHT isomer since it is predicted to generate three times more signals than the HHT isomer. In the L^{AB2} spectrum, the signals have almost equal intensity. Also seen in this region are the signals of protons H1 and H3, both in ortho positions to the NEt_2 substituent.

A second example is given in Figure 5 (top and middle) where the region of the aryl protons is shown for $La_2(L^{AB2})_3$ and $Lu_2(L^{AB2})_3$. In this spectral range, the only triplets are of H16 (as determined by comparison with spectra of L^{AB1}) and it is clear that there are one single signal from the HHH isomer and three signals from the HHT isomer. The percentages of HHH isomers have been calculated from integrated signal intensities in the NMR spectra and are given in Table 3.

Signals in the heterobimetallic spectra have been assigned with the aid of the corresponding homobimetallic spectra. In Figure 5 is shown the spectrum of $LaLu(L^{AB2})_3$ together with spectra of the two corresponding homobimetallic complexes. A second example is given in Figure 6 (bottom), where NMR signals of a solution with overall stoichiometry $LaCe(L^{AB3})_3$ are shown with assignment. Apart from signals of the two homobimetallic complexes, the small difference in size between the two Ln^{III} ions gives rise to appreciable amounts of both HHH-$LaCe(L^{AB3})_3$ and HHH-$CeLa(L^{AB3})_3$ in which the positions of the two ions in the coordination sites are switched. The attribution of NMR signals to the latter complex is based on the assigned spectrum of the HHH-$CeLu(L^{AB3})_3$ helicate since both these complexes contain a paramagnetic Ce^{III} ion in the bpb coordination site and a diamagnetic (La^{III} or Lu^{III}) in the bpa site. A more detailed analysis of the NMR spectra of paramagnetic complexes of

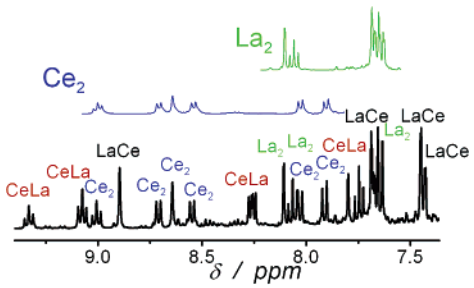

Figure 6. Aromatic region of the 400 MHz ^{1}H NMR spectra of $La_2(L^{AB3})_3$ (top), $Ce_2(L^{AB3})_3$ (middle), and a solution with overall stoichiometry La/Ce/L^{AB3} = 1:1:3 (bottom).

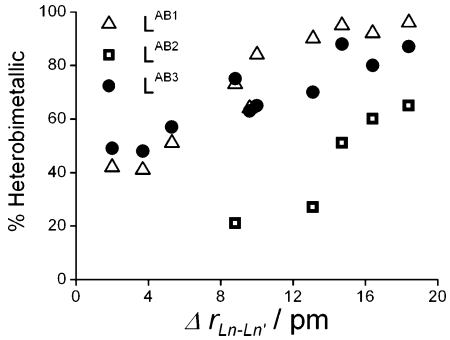

Figure 7. Percentages of heterobimetallic complexes versus difference in ionic radii.

L^{AB2} and L^{AB3} including the relationship between the lanthanide-induced shift and the solution structure will be published separately.

Percentages of the different species are given in Tables S9 and S10 (Supporting Information). Total heterobimetallic percentages are illustrated in Figure 7. As can be seen, the two ligands both exhibit nonstatistical behavior, although in different ways. L^{AB3} exhibits behavior similar to L^{AB1} with the percentages of heterobimetallic complexes being close to the statistical value (50%) for pairs of lanthanide ions with similar size (e.g., LaCe) and approaching 90% for the LaLu couple. The complexes of L^{AB2} are markedly different. For the LaLu couple, the percentage of heterobimetallic complexes is only 65%, a value that falls to 21%, well below the statistical value, for the EuLu couple.

Discussion

The complexes with different Ln^{III} ions have remarkably similar structures. Values of helical pitch and Ln−Ln′ distance do not vary significantly along the lanthanide series. The only differences to be found are the Ln−X distances, which follow the usual lanthanide contraction trend, and the angle ω, which describes the twist of the upper and lower faces of the trigonal prism of the coordination polyhedron with respect to each other. The value of interstrand ω decreases from 15° to 10° in going from Ce to Lu, indicative of a tighter wrapping of the ligand strands around the smaller Ln^{III} ions. The three helically wrapped ligands can thus be considered to form a rather rigid receptor for a pair of Ln^{III} ions, irrespective of the nature of the metallic ions. In monometallic complexes with related benzimidazole-pyridine-benzimidazole ligands, $\pi-\pi$ stacking interactions be-

tween aromatic groups on adjacent ligand strands contribute to the stability of the complexes, as judged from the short distances between the ring systems. In the complexes with L^{AB3}, on the other hand, the distances are longer ($\geq$3.5 Å), meaning that these interactions only play a smaller role. Despite numerous experiments, no crystals of sufficient quality for X-ray diffraction have been isolated for complexes with L^{AB2}. This could be related to the high percentages of HHT complexes, which will not pack with HHH molecules.

For the homobimetallic Ln_2L_3 complexes in acetonitrile solution, both ligands exhibit behavior deviating from statistical values when it comes to the percentages of the HHH and HHT isomers. For L^{AB2}, the HHH isomer is found in 6−20% yield, depending on the Ln^{III} ion, and the corresponding values are 79−87% for the L^{AB3} complexes. As for the helicates with ligand L^{AB1}, the percentage of HHH species is clearly related to the ability of encapsulating a heteropair of lanthanide ions. This is consistent in that a HHT arrangement of the ligand strands results in less difference in the two coordination cavities and therefore in less selective complexation.

In solutions of overall heterobimetallic stoichiometry, L^{AB3} behaves similarly to L^{AB1}. For pairs of Ln^{III} ions with similar size, the proportion of heterobimetallic complexes is close to the statistical value of 50%. Upon increasing the size difference, this proportion increases to 87% for the LaLu couple. The complexes with L^{AB2}, on the other hand all give lower heterobimetallic percentages, reaching only 65% for the LaLu couple. The large percentages of HHH for the L^{AB3} complexes and henceforth the better selective binding when compared to L^{AB2} is affected by several causes, not necessarily convergent, and with the data presently at hand, it is difficult to trace them out quantitatively, especially that the energy differences involved are small ($\approx$5 kJ·mol^{-1}). A first factor is the small differences in the large ion−dipole Ln−X interactions which are the strongest interactions keeping the metal ions inside the structure. The strength of these interactions is indeed modulated by the substituent R, and the electron-donating diethylamine group of L^{AB2} grafted in this position was expected to enhance the coordination ability of the tridentate bpa unit, resulting in a better coordination of the lanthanide ion with the smallest ionic radius. In fact, a reverse situation is observed, which may be interpreted as the tridentate unit in L^{AB2} being now too strongly coordinating to discriminate between lanthanide ions. A similar situation was encountered with a ligand in which the diethylamide unit of the bpa coordination site is replaced by a carboxylic acid function, known to be a very strong complexation agent for lanthanide ions.[29] On the other hand, the bpa coordinating unit of L^{AB3} has been far less modified by the chlorine substituent, and as a result, the performance of ligand L^{AB1} is almost fully regained. The second factor is the difference in interligand interactions, for instance between the weak interstrand $\pi-\pi$ interactions, the HHH isomer being possibly more stabilized by these interactions; the lack of structural information available on HHT complexes of L^{AB3}, however, precludes an in-depth discussion. Finally, solvation differences between the two isomers may also play a role. On the other hand, it is not expected that the otherwise large electrostatic repulsion energy between the two trivalent ions will be significantly different between the two isomers, unless the intermetallic distance changes substantially.

Conclusion

Altogether, it has been demonstrated here that the HHH $\rightleftarrows$ HHT equilibrium can be tuned by the nature of the substituent in the 4-position of the pyridyl group. The importance of this equilibrium is underlined by the data on the heterobimetallic complexes, the proportion of heterobimetallic species paralleling the proportion of HHH isomer. The tuning is extremely sensitive to slight variation in the donor strength of the bpa coordinating unit and this gives a fascinating tool to synthetic chemists to direct the self-assembly process of such helicates. The different factors contributing to the stabilization of one of the "selective" isomer still remain to be quantitatively deciphered. Work is currently being carried out in order to gather quantitative information on the energetics of the HHH $\leftrightarrows$ HHT equilibrium and, henceforth, on the origin(s) of the selective insertion of a heteropair of lanthanide ions into the helical structures studied here.

Acknowledgment. This project is supported through grants from the Swiss National Science Foundation.

Supporting Information Available: X-ray crystallographic files in CIF format for the four structures presented combined in a single file, scheme for the synthesis of **4**, tables with NMR data for the ligands in chloroform, elemental analyses of the complexes, analysis of the coordination polyhedra and interplanar angles, and a figure for the definition of angles in the coordination polyhedra. This material is available free of charge via the Internet at http://pubs.acs.org.

IC0608501